8TH ARTICLE

Electrochemical detection of hydrogen uptake in electrodeposited nickel/ nickel hydroxide system to prevent corrosion process

G.A. Santos[1], A.G.S.G. Silva[2], L.S.Sanches[2], H.A.Ponte[2]; C.E.B. Marino[1] claudiamarino@ufpr.br +55 41 3361-3129 (phone/fax)

1 – Department of Mechanical Engineering, Federal University of Paraná, CP 19011-CEP 81531-990, Curitiba/PR, Brazil
2 – Department of Chemical Engineering, Federal University of Paraná, CP 19011-CEP 81531-990, Curitiba/PR, Brazil

Keywords: nickel; electrodeposition; hydrogen detection, corrosion; surface properties

ABSTRACT

Brazil has been emphasizing the processing of heavy oils with high corrosivity. This deterioration involved the hydrogen permeation. Electrochemical techniques were used to study the behavior of nickel electrodeposited on a stainless steel during hydrogen charging cycles. The variation of the electrochemical parameters, such as the open-circuit potential indicates the possible presence of hydrogen in the electrodeposited nickel. The XRD analyses show a stable electrode before and after the hydrogen charging cycles. This methodology was efficient for the detection of hydrogen in its early stages of incorporation into the electrode and for the detection of chemical interactions with metallic structures.

*Corresponding author: claudiamarino@ufpr.br; phone/fax number +55 41 3361-3129UFPR: Jardim das Américas, CP 19011, 81531-990, Curitiba, PR, Brazil

1. INTRODUCTION

Hydrogen is one of the most harmful species in various metals and their alloys. Consequently, the quantification of this element in metals and alloys is necessary to understand and prevent hydrogen embrittlement [1]. In recent years, several materials have been investigated as electrochemical hydrogen sensors based on the method of Devanathan and Stachurski[2]. Some of these sensors have exhibited good sensitivity; however, others have demonstrated that they are not suitable as sensors because of problems related to irreversibility processes, oxide formation, stoichiometric variations and response time. In permeation processes, knowing the mechanism and the intensity of hydrogen permeation across metallic membranes is critical. These membranes, when investigated as sensors, are usually selected based on their high permeability and their high selectivity to hydrogen [3,4]. Various research groups have studied hydrogen permeation in materials that contain iron [5]. When iron and/or steel are investigated, coatings of nickel and palladium are commonly applied to the detection surface. These coatings have two functions: to avoid iron oxidation and to increase the efficiency of the hydrogen oxidation reaction. A nickel film electrodeposited under iron or steel across nickel sulfate and nickel chloride solutions represents an excellent alternative to the use of palladium [6]. Hillier *et al*. used the technique of metal electrodeposition to study hydrogen permeation; they used a substrate of AISI 4340 metal covered with electrodeposited zinc and cobalt and determined the hydrogen permeation using the Devanathan–Stachurski technique [7]. Within this context, this work was aimed at investigating the electrochemical behavior of nickel electrodeposited on AISI 316 stainless steel under cyclic hydrogen charging across the variation of electrochemical potentials.

2. MATERIALS AND EXPERIMENTAL PROCEDURES

The experiments were performed using a three-electrode cell made of glass, with a capacity of 100 mL; the cell contained a reference electrode (saturated calomel – SCE, Hg/Hg_2Cl_2, sat. KCl), a working electrode with a 1cm² area and an auxiliary platinum electrode that consisted of platinum foil with an approximate area of 1 cm². Nitrogen gas with a purity of 99.996% was bubbled through the solutions to de-aerate them. The electrolyte was a 0.1 $mol.L^{-1}$ NaOH (to ensure the chemical stability of nickel surface) maintained at a temperature of approximately 22°C. Before each experiment, the solution was deaerated by bubbling

with nitrogen gas for 15 minutes. The working electrode was fabricated using a galvanostatic electrodeposition technique; AISI316L (C 0.025; Si 0.012; Ni 10.4; Mn 1.4; Cr 16.6; Mo 2.11; N 0.078; P 0.039; S 0.025 wt%) stainless steel mesh was used as a substrate. This substrate (working electrode) had dimensions of 10×12 cm^2 and was cleaned with distilled water and immersed in hydrous ethanol for 30 minutes. The electrolyte used for the electrodeposition was composed of 240g/L $NiSO_4.6H_2O$, 30g/L $NiCl_2$. $6H_2O$ and 30g/L H_3BO_3 (*Watts* bath-pH 3.8) with analytical-grade reagents. During the electrodeposition process, the system was maintained at 60±2°C. The applied cathodic current density was 50mA/cm^2 and was generated by a power source [Powerbras 220Vca, 60cc and 0~30A]. The anode consisted of a platinum grid. The electrodeposition process required 40 minutes and thickness estimated around 41 μm from Faraday`s Law. Afterwards, the working electrode was cut to a length and width of 1 cm each for the electrochemical studies of hydrogen permeation. Cyclic voltammetry, open-circuit potential (OCP) and chronopotentiometry experiments were performed with a Voltalab 301 HGZ using the VoltaMaster software. In an initial experiment, the open-circuit potential was determined after 50 minutes. Six experiments were performed under open-circuit conditions and were alternated with five chronopotentiometry experiments using the same electrode. The current density and cathodic current in the galvanostatic polarizations were 40 mA/cm^2, 60 mA/cm^2 or 80 mA/cm^2 with a charging time of 10, 20 or 30 minutes; these experiments were used to evaluate the potential displacement with an increasing the number of cycles and the relationship between the potential displacement and hydrogen permeation. A cyclic voltammetry technique was used before and after the hydrogen charging cycles. The voltammograms were performed at a scan rate of 10 mV/s in the potential range between -1.5 V and 1.0 V using the same system. SEM (Scanning Electron Microscopy) micrographs were collected to characterize the electrode surface before and after successive hydrogen charging cycles. The SEM micrographs were collected on a JEOL model JSM 6360 LV scanning electron microscope. X-ray diffraction experiments were performed on a Shimadzu model XRD-6000 equipped with a CuKα (λ = 1.5418 Å) radiation source; the instrument was operated at a voltage of 40kV, a current of 40 mA and a scan speed of 0.2° min^{-1}.

3. RESULTS AND DISCUSSION

3.1 Voltammetry study

In view of the changes that can occur at the surface of the working electrode, voltammetric analysis was performed before and after hydrogen charging to identify any change in electrochemical behavior. Figure 1 presents the cyclic voltammogram of the electrode before and after all successive hydrogen charging cycles.

To obtain a better understanding of the changes, the voltammetric profiles were divided into three regions: (A), (B) and (C). Analysis of region (A) of the graphic (I), which represents the anodic part between the potentials from -1.5V to - 0.5V, revealed a peak (a') at approximately -1.0 V. This peak was assigned to the formation of α-$Ni(OH)_2$ according to the following reaction (1) [8-11]:

$$Ni + 2OH^- \rightarrow \alpha\text{-}Ni(OH)_2 + 2e^- \quad \textbf{(I)}$$

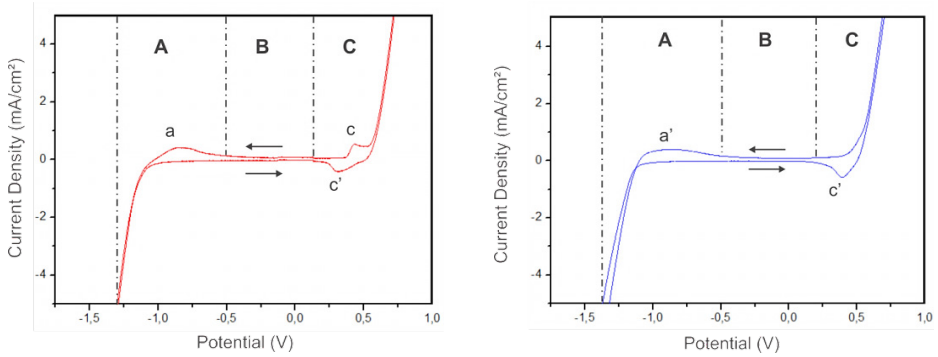

Figure 1. Cyclic voltammograms of the electrode in 0.1 mol/L NaOH solution and pH 13, before (I) and after (II) hydrogen charging cycles, between potentials from -1.5 V to 1.0 V, with scan rate equal to 10 mV/s.

In the same region, between the potentials from -1.5 V to -1.0 V, the cathodic part of the curve contains a peak attributable to the hydrogen evolution reaction (HER). Nickel hydroxides exhibit different structural forms in their oxidized and reduced states. Nickel hydroxide can therefore exhibit two polymorphs, identified as α and β.The structural difference between these polymorphs is the packing order along the crystallographic axis c in the β structure and a disordered packing order in the α structure, in which water molecules and anions occupy spaces between the layers. The different phases of nickel hydroxide were initially proposed by Chen [12]. The β structure exhibits a space of 4.8 Å between layers, whereas the layer spacing in the α structure is 8.0 Å [13-16]. Region (B) of the voltammogram anodic sweep in Figure 1 is associated with the passivation layer formed by α-$Ni(OH)_2$. In the anodic portion of region (C), between potentials of 0.25 V and 0.75 V, peak (c) is observed at 0.4 V. This peak represents a change in the oxidation state. In this potential region, $Ni^{2+}$from the species β-$Ni(OH)_2$, which forms from electrodeposition process, is oxidized to $Ni^{3+}$to form β-NiOOH according to the following reaction (2) [17,18]:

$$\beta\text{-}Ni(OH)_2 \rightarrow \beta\text{-}NiOOH + H^+ + e \quad \textbf{(2)}$$

With the oxidation of Ni^{2+} to Ni^{3+}, the release of oxygen between 0.75 V and 1.0 V is observed. In the cathodic sweep, in the potential range between 0.25 V and 0.75 V, it was possible to verify the reduction peak of Ni^{3+} to Ni^{2+} in the peak (c') at approximately 0.30 V, which arises from both β-$Ni(OH)_2$ and α-$Ni(OH)_2$ [11,19]. The α and β hydroxides are formed during the oxidation simultaneously with metallic nickel, Ni^0, during the electrodeposition process. This deposition layer is homogeneous, but irregular. After all of the hydrogen charging cycles, the stability of the system was evaluated according to the voltammogram (II) in Figure 1 [20], which was collected using the same working electrode. Analysis of the anodic part of region (A) in the voltammogram revealed that this region remained unchanged. The peak current (I_p) and the anodic charge density did not exhibited significant variation with respect to the formation of α -$Ni(OH)_2$ between the potentials of -1.1 V and -0.5 V. Thus, the results were an Ip value of 0.40 mA/cm² and a Q of 151.2 μC/cm² before the charging cycle and I_p and Q values of 0.38 mA/cm² and 120.5 μC/cm², respectively, after all of the hydrogen charging processes.

In the anodic portion of region (C) in Figure 1 (II), in the potential range between 0.25 V and 0.75 V, the peak related to the oxidation of Ni^{2+} to Ni^{3+} with a charge density of102.72 μC/cm² was not observed. Thus, the higher cathodic load occurs because, after the successive hydrogen charging cycles, every α-$Ni(OH)_2$ and β-$Ni(OH)_2$ generated during the electrodeposition process was reduced to Ni^0. When voltammetric analyses were performed after the charging (Figure 1 (II)), only the formation of α-$Ni(OH)_2$was observed in the potential range from -1.0 V to -0.75 V; the formation of the hydroxide resulted in the formation of a film on the surface. The peak at 0.37 V in the cathodic sweep in Figure 1 (II) is associated with the reduction of Ni^{3+} to Ni^{2+} [11,21].These profiles already were described in literature, accordingly.

3.2 Variation in the open-circuit potential with hydrogen charging

The open-circuit potential (OCP) data performed to determine the stabilization time of the system in a 0.1 mol.L^{-1}NaOH solution and to analyze the effects of hydrogen on the surface of the material. Before each hydrogen-charging process, an open-circuit potential experiment (Cycle 0) was performed to determine the OCP value under the initial electrode conditions. In the first step of the experiment, a stable open-circuit potential was achieved after 50 minutes (Cycle 0); after 50 minutes, the hydrogen charging cycle was performed with a cathodic current density of 40 mA/cm², 60 mA/cm² or 80 mA/cm² for 10 minutes, alternated with measurements of the open-circuit potential. An analysis of Figure 2 reveals the variation between the open-circuit potential and time, which shows a tendency toward stabilization at more negative potentials between Cycles 1 and

5. This tendency indicates that a change occurred in the superficial conditions of the electrode after hydrogen charging. This variation to more negative values might be associated with the hydrogen adsorption and absorption processes at the surface, and it might also indicate an initial stage of hydrogen incorporation. A comparison of Figures 2 (a), (b) and (c) indicated that, irrespective of the applied cathodic current density, the potential tends toward more negative values under these conditions when the same electrode is used, and the difference between the potentials of Cycles 1 and 5 is extended at higher current densities. The variation under an applied current density of 60 mA/cm² was Δ=0.153 V, whereas the variation under an applied current density 80 mA/cm² was Δ=0.220 V. These results indicate that higher current densities resulted in more extensive interaction between hydrogen and the surface of the material. The tendency of the open-circuit potentials toward more negative values under different cathodic current densities may be associated withthe incorporation of hydrogen into the octahedral interstices of the material and with the adsorption/absorption of hydrogen in the material [22].

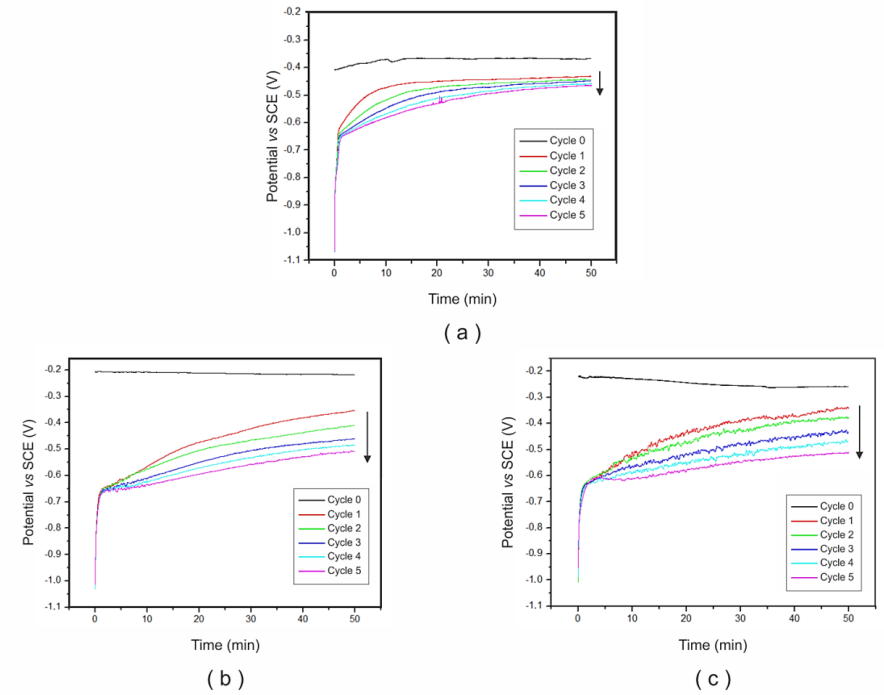

Figure 2. Open circuit potential of NiM316 electrode in 0.1 mol/L NaOH solution, with pH=13 at 22 °C, after chronopotenciometry during 10 minutes for which hydrogen charging cycles, on cathodic current densities of (a) 40 mA/cm², (b) 60 mA/cm² and (c) 80 mA/cm².

The hydrogen embrittlement occurs because of direct or indirect absorption in the defects of the metal-crystalline structure, which leads to the storage of

hydrogen [23]. However, a chemical reaction to produce hydride can also occur because of the high hydrogen absorption in metals and alloys such as palladium, nickel, titanium, and others [24]. These processes lead to changes in the open-circuit potential values, as observed in these results, because hydrogen interacts with nickel species in its atomic, molecular and ionic forms. Analyses of Figures 2 (a), (b) and (c) allowed to verify the tendency toward less-negative values relative to the initial open-circuit potential (Cycle 0) with the same electrode was used. This variation of the potential in Cycle 0 for different experiments may be associated with the reduction of Ni^{2+} to Ni^{0}at the electrode surface during the cathodic charging process. This reduction process was confirmed after the analysis of the voltammetric sweep presented in Figure 1 (II) after the completion of the cyclic hydrogen charging phase that did not exhibit the oxidation peak of the β-$Ni(OH)_2$ phase. Figure 3 presents the variation in the potential after each cyclic hydrogen-charging process under each set of experimental conditions.

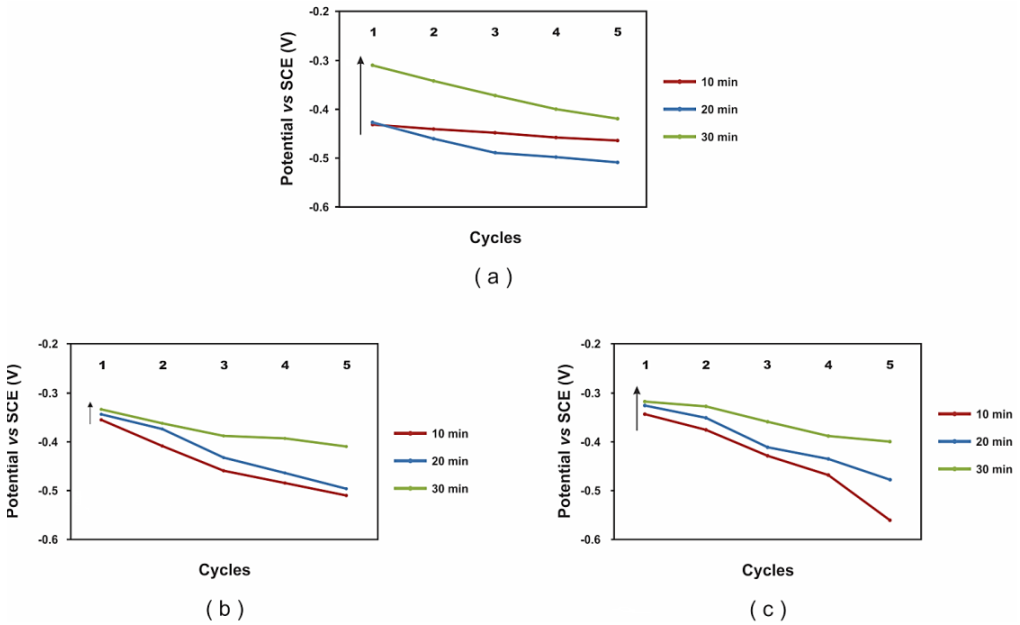

Figure 3. Variation of open circuit potential of the NiM316 electrode in 0.1 mol/L NaOH solution, with pH = 13 at 22ºC, on cathodic current densities of (a) 40 mA/cm², (b) 60 mA/cm² and (c) 80 mA/cm².

As analyzed previously in the Figure 2 profiles, a variation in the potential toward more negative values was observed between the initial and final cycles, irrespective of the cathodic current density and of the hydrogen charging time. With respect to the variation in the open-circuit potential (OCP), the Nernst equation ($E=E_0+2.3RT/\eta F.\log H^{+}_{ox}/H^{0}_{red}$) predicts that the application of a cathodic current density in the electrode surface will induce a decrease in the potentials toward more-negative values. This result might be associated with the reduced hydrogen

production rate, which is inversely proportional to the measured potential of stabilization.

A smaller variation in the potentials between Cycle 1 and Cycle 5 was observed under a cathodic current density of 40 mA/cm² and 10 minutes of charging time (Figure 3 (a)). This variation is associated with the decreased hydrogen production rate at the electrode surface. At this current density, the greatest variation was observed between the Cycle 1 results for the three charging times, which may be associated with the adsorption of hydrogen onto the electrode surface.

When the same electrode was used at a cathodic current density of 60 mA/cm², (Figure 3 (b)), the variation between potentials of Cycles 1 and 5 decreased to $\Delta = |0.075\ V|$ during hydrogen charging for 30 minutes; this results indicates that hydrogen may be retained in the irreversible adsorption sites and thereby induce saturation because of the use of the same electrode in the evolution hydrogen process. This beginning of the saturation process was further evidenced at a cathodic current density of 80 mA/cm² (Figure 3 (c)), where greater variations in the potentials between Cycles 1 and 5 at charging times of 10 minutes ($\Delta = |0.220|$ V) and 20 minutes ($\Delta = |0.153|$ V) were observed, along with a smaller variation at a charging time of 30 minutes ($\Delta = |0.084|$ V).

Another important parameter that should be analyzed during the investigation of a system to be used as a sensor is the reversibility. Analysis of only Cycle 1, as marked in Figures 3 (a), (b) and (c), at each cathodic current density for the three different charging times, allowed us to verify that the potentials tends toward less-negative values. This result indicates good reversibility of the interaction process with hydrogen. This hydrogen may be retained in the reversible traps of the microstructure because of the use of the same electrode in different experiments. These traps are known as crystalline defects and include grain boundaries and dislocations [25].

3.3 Structural and surface studies

3.3.1 Morphological analysis

A *Watts* bath was used in the electrodeposition process for AISI316L stainless steel to analyze the chemical and electrochemical characteristics of nickel with respect to hydrogen permeation. After this electrodeposition (Fig. 4(a)), the surface morphology was uniform and homogeneous in the agglomerate form, which indicated the presence of deposits [24].

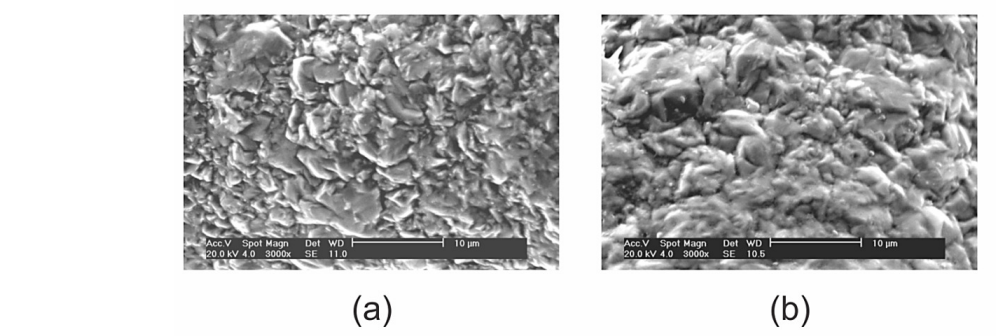

Figure 4. SEM micrograph of the electrodeposited nickel: before (a) and after (b) hydrogen charging (3000x).

After the same electrode surface was subjected to successive hydrogen charging cycles at different cathodic current densities, the surface was re-examined. Figure 4 (b) shows a deposit that remained intact, which indicates that the agglomerated form was maintained in a homogeneous distribution.

3.3.2 Surface analysis by x-ray diffraction (XRD)

The nickel species can react with hydrogen to produce metallic hydrides [26]. Two types of hydrides are formed: α-NiH and β-NiH. These hydrides are known to be obtained during cathodic charging or when nickel is saturated with hydrogen under high gas pressure [27]. To characterize the Ni-H bonding in the microstructure, the samples were analyzed by X-ray diffraction before and after the successive hydrogen-charging cycles (Figures 5 (a) and (b)).

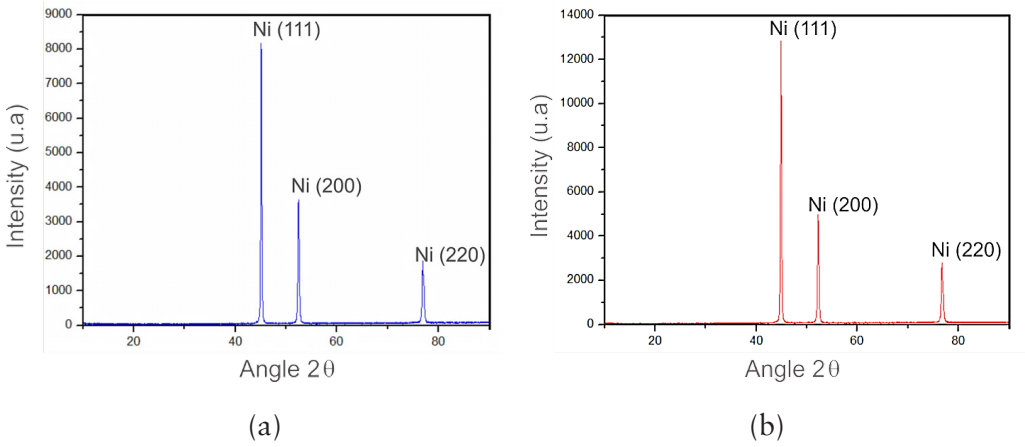

Figure 5. X-ray spectrum of the surface electrode: before (a) and after (b) the hydrogen charging cycle.

The x-ray diffraction spectra, it was possible to clearly observe reveal peaks related to metallic nickel in the face-centered cubic (FCC) phase. In the Figure 5

(a) the peaks at 2θ angles of 45.08° and 52.40°are related to the (111) and (200) planes, whereas the (220) plane is indicated by the peak at 76.86° [24,28,29]. After the successive hydrogen charging cycles, an increase in the intensity of the peaks related to the crystallographic Ni (111), (200) and (220) plane was observed according to the spectra shown in Figure 5 (b), which represents the analysis of the electrode surface that contained electrodeposited nickel [16,30-32].

This increase in the intensity might be associated with the reduction of β-$Ni(OH)_2$at the surface of the electrode that contained electrodeposited nickel, which would resulted in an increase in the crystallinity of the deposited metallic nickel. The spectra in Figure 5 do not show peaks related to the formation of hydrides, which might be attributable to the instability of β-$NiH_{0.7}$ at room temperature and atmospheric pressure. Thus, as nickel hydrides are not necessarily crystalline and could not be detectable by XRD would be necessary to study the surface chemistry of these materials by X-ray photoelectron spectroscopy or secondary ion mass spectrometry.

4. CONCLUSIONS

The influence of hydrogen on the electrochemical behavior of electrode surfaces with electrodeposited nickel was investigated. According to the characteristics of the open-circuit potential (OCP) curves measured after successive charging cycles, the surfaces of the electrodes exhibited important variations in potential in response to the cathodic reduction of hydrogen at the surface of the electrodes during the initial charging stages. The sensitivity of this electrode potential was confirmed by its variation between the first and the last hydrogen-charging cycle at three different cathodic current densities. The characterizations of the morphology and composition of the electrode surface compositions confirmed that the surface electrode that contained electrodeposited nickel did not undergo changes related to the process of hydrogen charging. Based on X-ray diffraction results, we concluded that the nickel electrode is not subjected to microstructural changes. Thus, this work suggests that electrodeposited nickel electrodes could be used as an active matrix for electrochemical sensors about the detection of the hydrogen chemical incorporation on the metallic structures.

ACKNOWLEDGMENTS:

We thank PIPE-UFPR (Graduate Program of Materials Science and Engineering) and the *Brazilian Institute of Petroleum* (IBP) for financial support, collaborations and guidance for this research. Finally, we thank the CNPq productivity fellowship (Grant number 301434/2013-1) from Cláudia Eliana Bruno Marino.

REFERENCES

[1] T Zakroczymski, Electrochim. Acta 51 (2006) 2261.

[2] MAV Devanathan, Z Stachurski, The Royal Soc. 270 (1962) 90.

[3] K Yamakawa, M Ege, B Ludescher, M Hirscher, H Kronmuller, J. Alloys Comp. 321 (2001) 17.

[4] YJ Ouyang, G Yu, AL Ou, L Hu, WJ Xu, Corr. Sci. 53 (2011) 2247.

[5] H Addach, P Berçot, M Rezrazi, J Takadoum, Corr. Sci. 51 (2009) 263.

[6] C Azevedo, PSA Bezzera, F Esteve, CJBM, Joia, OR Mattos, Electrochim. Acta 4 (1999) 4431.

[7] EMK Hillier, MJ Robinson, Corr. Sci. 48 (2005) 1019.

[8] M Wu, K Chih, Int. J. Hydrogen Energy 36 (2011) 13407.

[9] MAC Domínguez, E Ramirez-Meneses, A Montiel-Palm, AMH Torres, HD Rosalesc, Int. J. Hydrogen Energy 34 (2009) 1664.

[10] HW Hoppe, HH. Strehblow, Corr. Sci. 31 (1990) 167.

[11] A Seyeux, V Maurice, LH Klein, P Marcus, J. Electrochem. Soc. 153 (2006) B453.

[12] CL Fang-Chen, CLY Chen-Qi, Trans. Nonferr. Met. Soc. 17 (2007) 654.

[13] K Provazi, MJ Giz, LH Dall´Antonia, SI Córdoba de Torresi, J. Power Sourc. 102 (2001) 224.

[14] U. Prakash, N. Parvathavarthini, RK Dayal, Intermetallics 15 (2006) 17.

[15] MS Kim, KB Kim, J. Electrochem. Soc. 145 (1998) 507.

[16] YW Li, JH Yao, CJ Liu, WM Zhao, WX Deng, SK Zhong, Int. J. Hydrogen Energy 35 (2010) 2539.

[17] NV Krstajic, VD Jovic, LJ Gajic-Kjrstajic, BM Jovic, AL Antozzid, GN Martellid, Int. J. Hydrogen Energy 33 (2008) 3676.

[18] E Shangguan, H Tang, Z Chang, X Yuan, H Wang, Int. J. Hydrogen Energy 36 (2011) 10057.

[19] KD Song, KB Kim, SH Han, S Lee, HK Lee, Electrochem. Comm. 5 (2003) 460.

[20] Y Wang, D Cao, G Wang, S Wang, J Wen, J Yin, Electrochim. Acta 56 (2011) 8285.

[21] Y Lia, J Yaoa, Y Zhua, Z Zoub, H Wang, J. Power Sourc. 203 (2012) 177.

[22] SSM Tavares, S Miraglia, D Fruchart, DS Santos, J. Alloys Comp. 347 (2002) 105.

[23] S. Frappart, A. Oudriss, X. Feaugas, J. Creus, J. Bouhattate, F. Thébault, L. Delattre, H. Marchebois, ScriptaMaterialia 65 (2011) 859.

[24] L Chao-Qun, L Xin-Hai, W Zhi-Xin, G Hua-Jun, Trans. Nonferr. Metals Soc. China 17 (2007) 1300.

[25] A Oudriss, J Creus, J Bouhattate, C Savall, B Peraudeau, X Feaugas, Scripta Materialia 66 (2012) 37.

[26] M Monev, Electrochim. Acta. 46 (2001) 2373.

[27] J Remigijius, A Selskis, V Kadziauskiene Electrochim. Acta 47 (2002) 13.

[28] JT Richardson, R Scates, MV Twigg, App. Cat. A: Gen. 246 (2003) 137.

[29] SSM. Tavares, S Miraglia, A Lafuente, D Fruchart, J. Magnet. Mat. 242 (2002) 898.

[30] D Kong, J Wang, H Shao, J Zhang, C Cao, J. Alloys Comp. 509 (2011) 5611.

[31] A Ul-Hamid, H Dafalla, A Quddus, H Saricimen, LM Al-Hadhrami, Applied Surface Science 257 (2011) 9251.

[32] A Godon, J Creus, X Feaugas, E Conforto, L Pichon, C Armand, C Savall, Mat. Charact. 62 (2011) 164.